Bionanotechnology

DOI: 10.1002/anie.201106102

Graphene Oxide Nanoparticles as a Nonbleaching Optical Probe for Two-Photon Luminescence Imaging and Cell Therapy**

Jing-Liang Li, Hong-Chun Bao, Xue-Liang Hou, Lu Sun, Xun-Gai Wang, and Min Gu**

The generalization of many optically based techniques relies on the development of efficient optical probes. For example, two-photon microscopy with a near-infrared (NIR) laser is a promising technique for early cancer detection and therapy owing to the lower background signal, deep tissue penetration (because of low Rayleigh scattering and low tissue absorption of NIR light), reduced photobleaching, and reduced phototoxicity.[1] While one-photon excitation uses simple continuous-wave lasers, two-photon excitation requires a high reflux of excitation photons, usually by a femtosecond laser. However, molecular dyes absorb light in the visible wavelength region, and their two-photon luminescence (TPL), induced by an ultrafast NIR laser, is very weak due to their small two-photon excitation cross-section. This, combined with the high toxicity and photobleaching of most molecular dyes, limits their applications. With regards to treatment, because of the multi-drug resistance of cancer cells, developing methods that eliminate the use of chemical drugs is desired. To this end, ultrafast NIR-laser-based microsurgery is a promising solution for noninvasive cancer treatment at early stages.[1b] However, it has not been adopted as a general technique for medical applications owing to safety concerns over laser usage. Because of the slight absorption of NIR light by tissue, the power and energy fluence used to produce therapeutic effects has to be very high. Therefore, a probe that is more photostable and biocompatible, and which can significantly reduce the laser power needed for imaging and therapy, is essential for the general application of two-photon microscopy.

Lately, graphene has been a hot topic due to recent achievements in its large-scale preparation.[2] Major attention has been focused on applications of graphene in electronics because of its remarkable electronic and mechanical properties.[3] In contrast, its potential applications in biological or biomedical fields have not been widely explored. As graphene is comprised of carbon, it should be superior to most of the nanomaterials currently being used or explored in terms of biocompatibility. The photoluminescence of graphene and its derivatives, such as graphene oxide (GO) and reduced graphene oxide (rGO), for optical imaging and therapy is becoming a subject of research.[4] However, most of this research is focused on the luminescence induced by continuous-wave lasers through one-photon excitation. Herein, it is demonstrated that strong photoluminescence from two-photon excitation can be induced in GO by an ultrafast pulsed laser. The application of this technique to cancer cell imaging, using a gastric cancer cell line (AGS) as an example, is also investigated along with the potential application of the photothermal effects of graphene oxide nanoparticles (GONs) for cancer cell therapy. We observed that intensive microbubbling can be induced by irradiation at a laser power as low as 4 mW in the presence of GONs, which causes instant cell damage.

GONs with sizes of around 30 nm (Figure 1 a) were prepared and functionalized with transferrin (Trf) molecules for TPL cell imaging and treatment. Transferrin has been proven to be an efficient ligand for targeting cancer cells, which overregulate transferrin receptors.[5] Polyethylene glycol (PEG) was also linked to GONs to stabilize the particles in cell culture buffers, as it has been shown that PEG

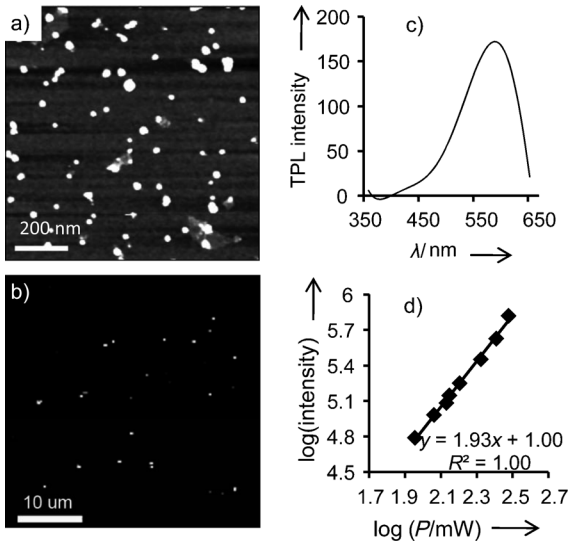

Figure 1. Characterization of graphene oxide nanoparticles (GONs). a) an AFM image of GONs; b) a TPL image of GONs deposited on a cover slip; c) a TPL spectrum of GONs (cut off at 660 nm by the cascading filters); d) a logarithmic plot of the TPL intensity as a function of laser power.

[*] Dr. J. L. Li,[+] X. L. Hou,[+] L. Sun, Prof. X. G. Wang
Centre for Material and Fiber Innovation, Deakin University
Waurn Ponds, Vic 3216 (Australia)
E-mail: xungai.wang@deakin.edu.au
Dr. H. C. Bao,[+] Prof. M. Gu
Centre for Micro-Photonics, Swinburne University of Technology
Hawthorn, Vic 3122 (Australia)
E-mail: mgu@swin.edu.au
[+] These authors contributed equally to this work.

[**] We would like to thank Dr. Xiangping Li for assistance with the TPL spectrum measurement, Dr. Luhua Li for assistance with AFM analysis, Mandy Ludford-Menting for help with cell preparation during the revision of this manuscript, and Prof. Saulius Juodkazis for helpful discussions.

Supporting information for this article is available on the WWW under http://dx.doi.org/10.1002/anie.201106102.

can prolong blood circulation of nanoparticles.[6] The molecular structure of the functionalized GO is shown in Scheme 1. The UV-visible absorption spectra of both the pristine GONs and those labeled with transferrin molecules are given in the

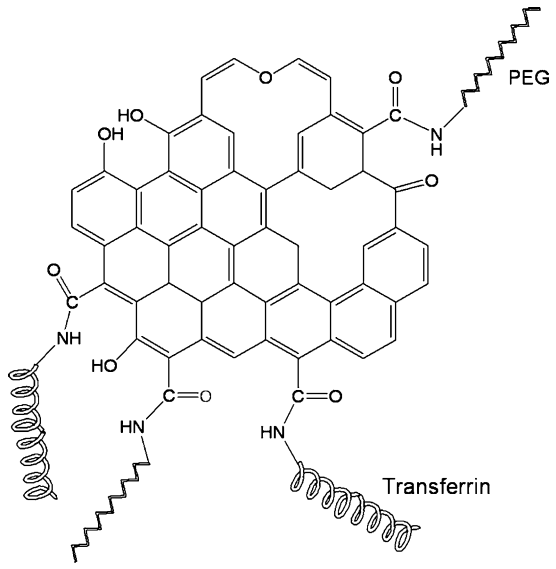

Scheme 1. A representation of the molecular structure of graphene oxide conjugated with transferrin and PEG.

supporting information (Figure S1). The spectra indicate the presence of protein molecules on GONs. We observed that GONs give strong photoluminescence under the irradiation of a short-pulsed laser (Figure 1 b). The photoluminescence spectrum is in the range of 400 to 650 nm, with the maximum located at 590 nm (Figure 1 c). A plot of the photoluminescence intensity versus the incident power on a logarithmic scale fits a straight line with a slope close to two (Figure 1 d), indicating that the photoluminescence is due to two-photon excitation. It is well-known that the TPL of molecular dyes and autofluorescence, which are conventionally used for cell imaging, is very sensitive to the excitation wavelength.[7] The search for novel markers with strong photoluminescence that can be excited with a wider range of wavelengths is of practical significance. The development of such a marker can enable great flexibility in choosing a laser. The range of TPL excitation wavelengths for GONs is quite broad. No significant change in the TPL intensity of GONs was observed when the wavelength was varied between 750 nm and 850 nm (Figure S2 in the Supporting Information). This is due to the weak wavelength dependence of light absorption in grapheme that is attributable to its continuous band structure. The weaker wavelength dependence is a feature of GONs, which distinguishes them from molecular dyes and cell autofluorescence. Furthermore, we observed that the TPL strength did not change much after the GONs were irradiated with a laser for an extended period of time (Figure S3 in the Supporting Information). This non-bleaching effect is another feature that makes GONs a superior optical probe to molecular dyes.

To demonstrate the capacity of GONs for cell imaging, the TPL of the GONs is compared with that of the cell autofluorescence and a conventional molecular dye, fluorescein isothiocyanate (FITC). A power as high as 35 mW has to be used to induce sufficient autofluorescence in the cells at the optimal excitation wavelength of 760 nm. To obtain enough fluorescence from FITC-transferrin, a laser power of 30 mW has to be applied at the optimal wavelength of 790 nm.[7] The high laser powers required to get sufficient autofluorescence and FITC signal are due to the low two-photon excitation cross section of the fluorescent molecules. In contrast, a low power of 7 mW is sufficient to induce strong photoluminescence in GONs on cells (Figure 2). To limit the detrimental effects of the laser on cells labeled with GONs, an area of 240 μm × 240 μm was scanned, which is three times the

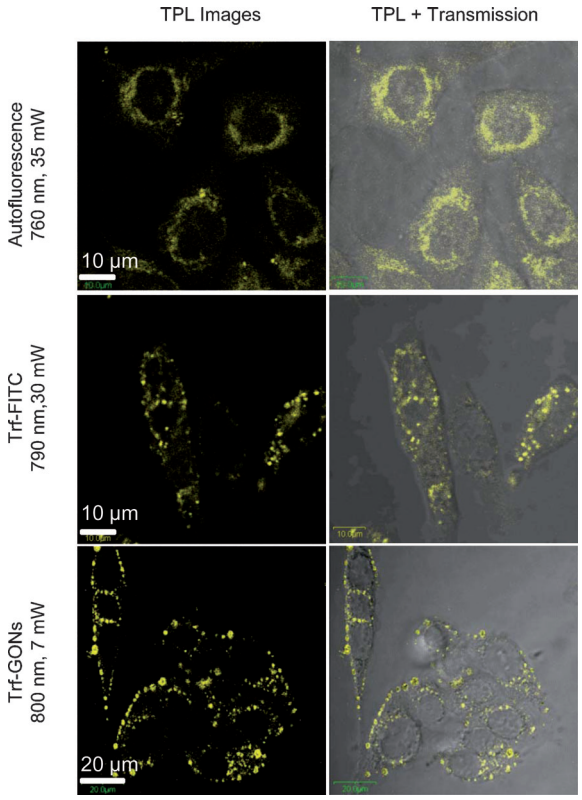

Figure 2. A comparison of the in vitro TPL of GONs with cell autofluorescence and molecular dye FITC.

area for treatment of cells. Since the time for one scan is fixed at one second, scanning a larger area reduces the exposure duration of GONs to the laser and thus reduces the photothermal effects of GONs.

Three-dimensional imaging of cells labeled with Trf-GONs was carried out in a collagen matrix. Collagen is generally used as a tissue phantom for in vitro studies. When labeled with GONs, cells in collagen as deep as 100 μm can be clearly imaged at an incident laser power of 7 mW (objective lens: 60×, numerical aperture (NA) 1.2, water immersion; Figure S4 in the Supporting Information). In contrast, when cells were labeled with Trf-FITC, we observed that a penetration depth of only 30 μm was achieved at an incident laser power of 30 mW. This comparison indicates that the

efficiency of GONs in terms of the laser power and penetration depth is at least one order of magnitude higher than that of the molecular dye FITC. When the objective lens is replaced with one (20×) with a lower numerical aperture of 0.4, cells labeled with Trf-GONs can be clearly imaged at a depth of 1 mm (Figure S4 in the Supporting Information).

When cells were labeled with GONs, cell membrane integrity could be compromised at a laser power an order of magnitude lower than for unlabeled cells. In the absence of GONs, the laser power has to be as high as 40 mW to induce instant cell damage/death (Figure 3, third row). No cell damage was observed at a laser power as high as 35 mW (Figure S5 in the Supporting Information). In contrast, when cells were labeled with GONs, a power as low as 4 mW was sufficient to cause cell death. As shown in the first row of Figure 3, when cells were raster-scanned at 4 mW, microbubbling (black dots) was induced instantly. After a couple of minutes, addition of ethidium bromide (EB) revealed staining on a majority of cells. Live cells are impermeable to EB, which only stains the nuclei of cells with a compromised membrane, indicating cell death. More intense membrane perforation was observed when the laser power was increased. For EB imaging, the laser power was reduced to 2 mW to prevent further damage to cells during imaging. The second row of Figure 3 shows cell damage at a laser power of 8 mW. The concentration of Trf-GONs (20 $\mu g\,mL^{-1}$) used in this work is low, which did not affect cell viability. Obvious toxicity was observed at a concentration of 250 $\mu g\,mL^{-1}$ and cell viability was reduced to about 50% when the concentration was increased to 500 $\mu g\,mL^{-1}$ (Table S1 in the Supporting Information). It has been reported that a graphene oxide concentration of up to 40 $\mu g\,mL^{-1}$ was not toxic to other cancer cell lines.[8] After laser exposure, the cells were imaged at a larger field of view (Figure 3, third column), which showed that the damaging effect was confined to the area exposed to laser irradiation. Thus, the introduction of GONs allows for highly localized treatment at low power. The photothermal effects of Trf-GONs on a normal cell line (skin cell line HFF) were also examined. We observed that instant cell damage was induced only when the laser power was as high as 11 mW, which is more than 2.5 times higher than the threshold for AGS cells (Figure S6 in the Supporting Information). The higher laser power required for HFF cells should be due to the lower cellular uptake of the particles by the cells. Because of their higher metabolic rate, transferrin receptors are generally upregulated on cancer cells. Higher cellular uptake of transferrin-conjugated nanoparticles by cancer cells has been demonstrated in many other works.[5] The difference in the laser power thresholds for cancerous and noncancerous cells can be further enlarged through the use of more specific cancer-targeting molecules.

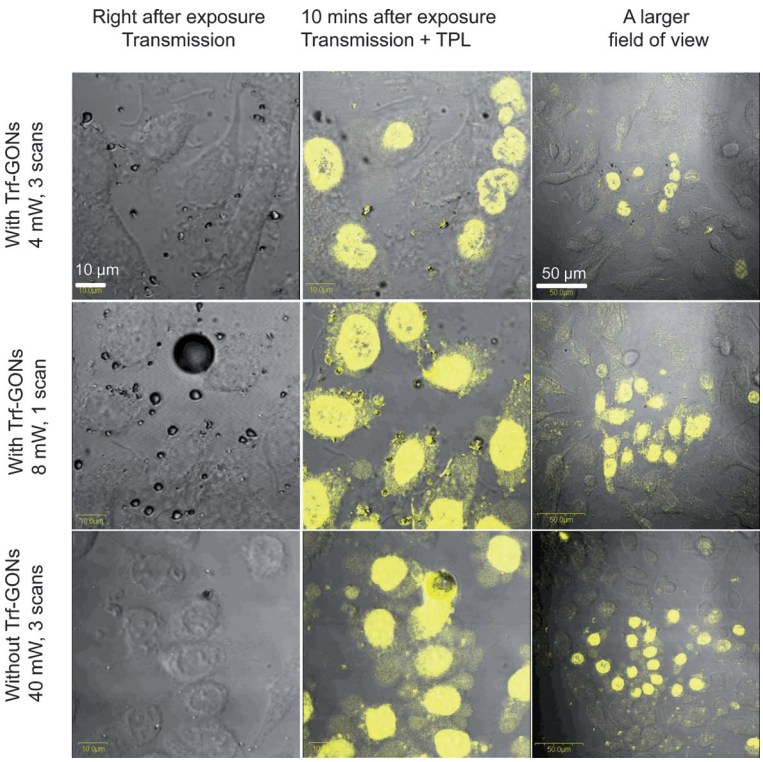

Figure 3. GON-enhanced cancer cell therapy.

The strong microbubbling observed in the presence of GONs is attributable to the instant heat production of the nanoparticles upon laser excitation. The irradiation of an ultrafast pulsed laser can generate a large amount of hot carriers with electrons in the conduction bands and holes in the valence bands through strong two-photon absorption (Scheme S1 in the Supporting Information). The temperature of the hot carriers can immediately jump to a few thousand degrees in about 50 femtoseconds from two-photon absorption. Those hot carriers recombine and release energy (a recombination time of about 1.2 picoseconds) through photoluminescence emission and carrier phonon scattering by collisions with the lattices in GONs, which causes the temperature rise in the lattices.[1c,7b] As the sizes of GONs are much smaller than the wavelength of the laser, it is reasonable to assume that energy loss from scattering is negligible. If we assume that all the energy is absorbed by the particles, on the basis of energy balance, the temperature rise ΔT of a particle can be estimated using Equation (1):

$$E = m\,C\,\Delta T = 4\pi/3\,R^3\,\rho\,C\,\Delta T \quad (1)$$

Where E is the absorbed energy of a particle, m is particle mass, R (15 nm) is the radius of a particle, ρ is the density of the material, and C is the heat capacity of the material. For the laser used in this work (pulse width 200 fs, repetition rate 80 MHz), the duration between two pulses is 12.5 nanoseconds, which is far longer than the temperature relaxation of graphene (0.5–1 ps).[9] This means that the energy absorbed from one pulse is released before the next pulse comes. It is thus reasonable to assume that E in Equation (1) equals the

energy of a single pulse. If we assume the density and heat capacity of GO are the same as that of graphite, then ρ and C are 2.1 $g\,cm^{-3}$ and 0.71 $J\,g^{-1}\,K^{-1}$, respectively.

For an average power of 4 mW, the peak pulse power is 250 W (4 mW/(80×10^6 Hz $\times$ 200×10^{-15} s)) and the energy of one pulse is 5×10^{-11} J (250 W $\times$ 200×10^{-15} s). According to Equation (1), this leads to a ΔT of 2.37×10^6 K. Since the particle size is significantly smaller than the spot size of the laser, a particle is exposed to only a small fraction of the total light ($(15\text{ nm}/400\text{ nm})^2 = 0.0014$, where 15 nm is the particle radius and 400 nm is the radius of the focus spot), which results in a reduction of ΔT to about 3300 K. Furthermore, considering that the light absorption of one single layer of graphene is 2.3 %,[10] it can be estimated that the total absorption of a particle with a diameter of 30 nm (ca. 30 layers) is 70 %. Therefore, the overall absorption of one particle is less than 0.1 % ($0.0014\times70\,\%$). Thus, the temperature increase of one particle can be about 2300 K. Such a high temperature increase can undoubtedly cause boiling and microbubbling of the water-based cell medium. The collapse of the microbubbles can produce high pressure shock waves that mechanically disrupt cell membranes and cause instant cell death (necrosis). The collapse of bubbles is evident from the significantly reduced number of bubbles after laser exposure (Figure 3, second column). Enhanced microcavitation has been regarded as a cause of cell death when gold nanoparticles are used.[11] We compared the microbubbling in the case of gold nanorods with that of GONs. Gold nanorods with an average size of 12 nm $\times$ 45 nm were used; their preparation and surface functionalization followed a known procedure.[12] At the same laser power, we observed that the microbubbling from gold nanorods was much weaker than that from GONs (Figure S7 in the Supporting Information). This was unexpected, as more intensive heat can be produced when gold nanorods are present, due to their strong surface plasmon resonance. Therefore, the microbubbling in the case of GONs may be contributed by other factors. It has been reported that graphene oxide can be reduced to graphene at moderate temperatures (100–250 °C).[13] Therefore, the temperature increase caused by laser excitation should be able to reduce graphene oxide. In this process CO_2 can be produced, which enhances the formation of microbubbles. In fact, after a few scans we observed that the TPL of GONs labeled on cells became stronger, thus suggesting that the reduction to graphene may occur. To verify this hypothesis, we measured the absorption of the GONs both before and after laser irradiation (Figure S8 in the Supporting Information). The absorption at visible wavelengths after irradiation is higher, which is also indicative of GON reduction. Interestingly, localized thermal reduction of graphene oxide with a heated atomic force microscope tip was achieved, which enables the nanoscale manipulation of the electrical properties of graphene materials for applications in microelectronics.[13] The heat produced by laser irradiation may also be used for the localized modification of graphene materials.

When the laser power was reduced to 3 mW, we observed that only a fraction of the cells in the scanning area were killed after 18 and 50 scans (Figure S9 in the Supporting Information). Further reduction of the laser power to 2 mW, instant cell death was not brought about when the cells were scanned 50 times (not shown). Microbubbling was not observed at these lower laser powers. It is worth mentioning that, although a further decrease in laser power does not cause significant cell necrosis, this does not mean that the therapeutic effects cannot be produced at a lower laser power. It has been demonstrated that heat shock can lead to cell death through apoptosis.[14] The determination of whether lower powers can induce cell apoptosis in the presence of GONs requires long-term cell monitoring after treatment, a subject worthy of further investigation.

Other types of nanoparticles, such as gold nanoparticles and carbon nanotubes, have also been investigated for cancer cell imaging and therapy owing to their photoluminescence and photothermal effects.[12,14b,15] However, gold is expensive, and the shape and size of a gold nanoparticle are very susceptible to laser irradiation, which reduces its photoluminescence.[16] The production of carbon nanotubes is also more expensive, and achieving a good dispersion of carbon nanotubes in an aqueous medium is a challenge. In contrast, GONs can be easily obtained by chemically exfoliating graphite. Interestingly, the application of the photothermal effects of rGO in cancer cell treatment was recently reported by other authors using a continuous-wave laser as an energy source.[8] With an unfocused laser beam, a high power of 15 $W\,cm^{-2}$ and a long duration of eight minutes were used to achieve therapeutic effects. The reduced irradiation duration for the femtosecond laser used in this work may be attributable both to the high peak pulse power of the laser and the ultrafast electron dynamics and more efficient energy absorption of the particles, which may find some similarity to the case when gold nanoparticles are used as photothermal agents.[15c]

In summary, GONs are shown to be a good optical probe because of their strong TPL. When cells are labeled with GONs, highly localized and low power/energy therapy can be achieved. The low cost and high efficiency of GONs combined with an ultrafast pulsed laser make GONs a promising material for three-dimensional two-photon imaging and laser-based cancer microsurgery. We also envision in vivo and biomedical applications through the integration of this technique with two-photon endomicroscopy. We recently demonstrated photothermal treatment with gold nanorods using endomicroscopy.[15b] Their aromatic molecular structure and the richness of their surface functional groups allow GONs to be functionalized with other targeting molecules, making them more specific in targeting different malignant tissues. In fact, the potential applications of GONs go far beyond what is explored in this work. For example, they can be potentially used for optically based molecular imaging, either for disease detection or other types of sensing. The photothermal effects may be also applicable to other treatments or processes where localized heating is required. Apart from cell ablation, the intensive microbubbling can also be used in other applications, such as void creation in materials, which is important to the fabrication of materials for applications in photonics and catalysis.

Received: August 29, 2011
Revised: October 13, 2011
Published online: January 13, 2012

Keywords: cancer · graphene oxide · imaging agents · photothermal therapy · two-photon luminescence

[1] a) W. Denk, J. H. Strickler, W. W. Webb, *Science* **1990**, *248*, 73 – 76; b) R. L. Amy, R. Storb, *Science* **1965**, *150*, 756 – 758; c) F. Helmchen, W. Denk, *Nat. Methods* **2005**, *2*, 932 – 940.

[2] a) D. Li, M. B. Mueller, S. Gilje, R. B. Kaner, G. G. Wallace, *Nat. Nanotechnol.* **2008**, *3*, 101 – 105; b) L. Jiao, L. Zhang, X. Wang, G. Diankov, H. Dai, *Nature* **2009**, *458*, 877 – 880.

[3] a) K. S. Novoselov, A. K. Geim, S. V. Morozov, D. Jiang, Y. Zhang, S. V. Dubonos, I. V. Grigorieva, A. A. Firsov, *Science* **2004**, *306*, 666 – 669; b) X. Li, X. Wang, L. Zhang, S. Lee, H. Dai, *Science* **2008**, *319*, 1229 – 1232.

[4] a) J. Shen, Y. Zhu, C. Chen, X. Yang, C. Li, *Chem. Commun.* **2011**, *47*, 2580 – 2582; b) X. Sun, Z. Liu, K. Welsher, J. T. Robinson, A. Goodwin, S. Zaric, H. Dai, *Nano Res.* **2008**, *1*, 203 – 212.

[5] a) J. L. Li, L. Wang, X. Y. Liu, Z. P. Zhang, H. C. Guo, W. M. Liu, S. H. Tang, *Cancer Lett.* **2009**, *274*, 319 – 326; b) P. H. Yang, X. S. Sun, J. F. Chiu, H. Z. Sun, Q. Y. He, *Bioconjugate Chem.* **2005**, *16*, 494 – 496.

[6] D. P. K. Lankveld, R. G. Rayavarapu, P. Krystek, A. G. Oomen, H. W. Verharen, T. G. van Leeuwen, W. H. De Jong, S. Manohar, *Nanomedicine* **2011**, *6*, 339 – 349.

[7] a) C. Xu, W. W. Webb, *J. Opt. Soc. Am. B* **1996**, *13*, 481 – 491; b) M. A. Albota, C. Xu, W. W. Webb, *Appl. Opt.* **1998**, *37*, 7352 – 7356.

[8] J. T. Robinson, S. M. Tabakman, Y. Liang, H. Wang, H. S. Casalongue, V. Daniel, H. Dai, *J. Am. Chem. Soc.* **2011**, *133*, 6825 – 6831.

[9] H. M. Dong, W. Xu, R. B. Tan, *Solid State Commun.* **2010**, *150*, 1770 – 1773.

[10] R. R. Nair, P. Blake, A. N. Grigorenko, K. S. Novoselov, T. J. Booth, T. Stauber, N. M. R. Peres, A. K. Geim, *Science* **2008**, *320*, 1308 – 1308.

[11] V. K. Pustovalov, A. S. Smetannikov, V. P. Zharov, *Laser Phys. Lett.* **2008**, *5*, 775 – 792.

[12] J. L. Li, D. Day, M. Gu, *Adv. Mater.* **2008**, *20*, 3866 – 3871.

[13] Z. Wei, D. Wang, S. Kim, S.-Y. Kim, Y. Hu, M. K. Yakes, A. R. Laracuente, Z. Dai, S. R. Marder, C. Berger, W. P. King, W. A. de Heer, P. E. Sheehan, E. Riedo, *Science* **2010**, *328*, 1373 – 1376.

[14] a) L. Tong, J. X. Cheng, *Nanomedicine* **2009**, *4*, 265 – 276; b) J. L. Li, M. Gu, *Biomaterials* **2010**, *31*, 9492 – 9498.

[15] a) L. R. Hirsch, R. J. Stafford, J. A. Bankson, S. R. Sershen, B. Rivera, R. E. Price, J. D. Hazle, N. J. Halas, J. L. West, *Proc. Natl. Acad. Sci. USA* **2003**, *100*, 13549 – 13554; b) M. Gu, H. C. Bao, J. L. Li, *J. Biomed. Opt.* **2010**, *15*, 050502; c) L. Tong, Y. Zhao, T. B. Huff, M. N. Hansen, A. Wei, J.-X. Cheng, *Adv. Mater.* **2007**, *19*, 3136 – 3141; d) J. W. Fisher, S. Sarkar, C. F. Buchanan, C. S. Szot, J. Whitney, H. C. Hatcher, S. V. Torti, C. G. Rylander, M. N. Rylander, *Cancer Res.* **2010**, *70*, 9855 – 9864.

[16] C. Ungureanu, R. Kroes, W. Petersen, T. A. M. Groothuis, F. Ungureanu, H. Janssen, F. W. B. van Leeuwen, R. P. H. Kooyman, S. Manohar, T. G. van Leeuwen, *Nano Lett.* **2011**, *11*, 1887 – 1894.

